

- (13) Dollan, F. E.; Briscoe, H. T. *J. Phys. Chem.* **1937**, *41*, 1129.
 (14) Rabinowitsch, A. J. *Z. Phys. Chem.* **1921**, *99*, 338.
 (15) Getman, F. H.; Gilroy, H. T. *Am. Chem. J.* **1912**, *48*, 138.
 (16) Lühdemann, R. Z. *Phys. Chem. Abt. B* **1935**, *B29*, 133.
 (17) Reilly, P. J.; Stokes, R. H. *Aust. J. Chem.* **1971**, *24*, 1361.
 (18) "International Critical Tables"; Washburn, E. W., Editor in Chief; McGraw-Hill: New York, 1928; Vol. III.
 (19) "Development of the Zinc Chloride Battery for Utility Applications"; EM-1417, Research Project 226-3 interim report; Electric Power Research Institute: Palo Alto, CA, May 1980; pp 37-2-37-4.
 (20) Agnew, A.; Paterson, R. J. *Chem. Soc., Faraday Trans. 1* **1978**, *74*, 2896.
 (21) Millero, F. J., University of Miami, Miami, FL, private communication, Jan 31, 1983.
 (22) Mills, R., Australian National University, Canberra, A.C.T., Australia, private communication, 1982.
 (23) Linke, W. F. "Solubilities of Inorganic and Metal-Organic Compounds", 4th ed.; ACS Publications: Washington, DC, 1965; Vol. II.
 (24) Linke, W. F. "Solubilities of Inorganic and Metal-Organic Compounds", 4th ed.; McGraw-Hill and Werner: Washington, DC, 1958; Vol. I.

Received for review March 10, 1983. Accepted August 30, 1983. This work was performed under the auspices of the U.S. Department of Energy by Lawrence Livermore National Laboratory under Contract No. W-7405-ENG-48.

Vapor-Liquid Equilibria for Three Aldehyde/Hydrocarbon Mixtures

Robert Eng and Stanley I. Sandler*

Department of Chemical Engineering, University of Delaware, Newark, Delaware 19716

Isothermal vapor-liquid equilibrium (VLE) data were measured for the mixtures *n*-pentane/propionaldehyde, *n*-heptane/*n*-butyraldehyde, and isobutyraldehyde/*n*-heptane at low pressures (100-1000 mmHg) by using a dynamic still. The data reported here are thermodynamically consistent according to the point-to-point consistency test. These data are correlated with five activity coefficient models with parameters estimated from the maximum likelihood method. Also, UNIFAC parameters were estimated for the aldehyde/hydrocarbon functional-group interactions based on the new data.

Introduction

Reliable experimental vapor-liquid equilibrium (VLE) data are of importance in the design of separation processes based on phase equilibria, and also to the continuing development of group contribution methods for the semitheoretical prediction of VLE.

In this study, isothermal VLE data were measured for the following binary systems: *n*-pentane/propionaldehyde at 40.0 °C, *n*-butyraldehyde/*n*-heptane at 45.0 and 70.0 °C, and isobutyraldehyde/*n*-heptane at 45.0 °C. Accurate data for these aldehyde/hydrocarbon systems, which have not been previously available, will allow for the revision of the UNIFAC parameters for the aldehyde/hydrocarbon functional-group interactions. These data will also be useful in developing a better understanding of polar-nonpolar interactions.

Few vapor-liquid equilibrium data have been published for aldehydes, an industrially important and common class of chemicals. The lack of such data may be attributed to the difficulty involved in working with aldehydes, due to their chemical instability to oxidation and polymerization (1).

Experimental Section

A crucial step in the experimental procedure was ensuring that the materials used were pure. Three physical properties (density, refractive index, and normal boiling point) were measured as a criterion of purity (2). The normal boiling point and the pure-component vapor pressure data are the most important and sensitive properties for determining purity. The pure-component vapor pressures of the same batch of chemicals as were used in the mixture experiments were measured with the Stage-Muller still to be described shortly, which was also

used for the binary VLE experiments. The vapor pressure data were correlated by using the Antoine equation

$$\log P = A - B/(T + C) \quad (1)$$

where the constants were determined by using the maximum likelihood method (3). The pure-component vapor pressures at the temperatures of interest are included in the experimental data sets which follow, and the Antoine constants appear in Table I.

n-Pentane and *n*-heptane were available in relatively high purity (99+%) from Alfa Products. Further purification was not necessary since no secondary peaks were found from gas-chromatographic analysis and physical property measurements proved satisfactory (see Table II). The aldehydes, also obtained from Alfa Products, were distilled in a packed, all-glass rectification column in a nitrogen atmosphere and stored over molecular sieves (Fisher, Scientific, M-514). Traces of an oxidation inhibitor, hydroquinone (<0.05 wt %), were added to the distillation charge to minimize any oxidation. The physical property measurements of the aldehydes are summarized in Table II. There was no evidence of polymerization or oxidation during the VLE experiments.

The vapor-liquid equilibrium experiments were the first that we have performed by using an all-glass, Stage-Muller dynamic equilibrium still (4), in which both the liquid and vapor phases are recirculated. The still was manufactured by Fischer Labor-und Verfahrenstechnik of West Germany. The essential features of the still, which have been described previously (4), are shown in Figure 1. The overall setup of the apparatus is shown in Figure 2. The important features of this still are the Cottrell pump, the silver-plated vacuum jacket, and the magnetic sampling valves. The jacket, which surrounds the equilibrium chamber, eliminates partial condensation of the vapor disengaging from the liquid at the exit from the Cottrell pump. The magnetic valves allow sampling without disruption of operation of the still. The still used in this study was further modified by adding condensers above the sampling points to recover any partially vaporized sample.

All experiments were carried out under an inert atmosphere of nitrogen (Matheson, purity greater than 99.99%) to avoid exposure to moisture and oxygen. The mixture was heated by immersing the boiling flask in a silicon oil bath. Mixing within the flask was accomplished by a magnetic stirrer. The temperature immediately outside the equilibrium chamber was maintained approximately 1 °C lower than the equilibrium temperature by using a thermostated heating jacket. Steady-state

Table I. Antoine Constants^a for Pure Compounds

compd	A	B	C	rmsd(ΔP), ^b mmHg	rmsd($\Delta P/P$)
<i>n</i> -pentane	7.572 42	1482.01	279.74	0.15	0.000 21
propionaldehyde	6.876 44	1055.479	216.18	0.27	0.000 38
<i>n</i> -heptane	6.783 81	1196.68	208.23	0.24	0.000 46
<i>n</i> -butyraldehyde	6.933 52	1181.71	216.79	0.31	0.000 61
isobutyraldehyde ^c	8.094 68	1868.82	294.56	0.20	0.000 43

^a $\log P = A - B/(T + C)$. ^b $\text{rmsd}(\Delta P) = [\sum_{i=1}^N (P_{\text{exptl}} - P_{\text{calcd}})^2 / (N - 3)]^{1/2}$. ^c Temperature range: 40–51 °C.

Table II. Physical Properties of Pure Compounds

property	this study	lit. ^a	% Δ ^b
<i>n</i> -Pentane			
$d_{4,20}^{20}$, g/mL	0.6260	0.6262	0.03
n_D^{20}	1.3575	1.35748	<0.01
nbp, °C	36.14	36.074	0.18
Propionaldehyde			
$d_{4,20}^{20}$, g/mL	0.7969	0.7970	0.01
n_D^{20}	1.3633	1.3619	0.10
nbp, °C	47.97	48.0	0.06
<i>n</i> -Heptane			
$d_{4,20}^{20}$, g/mL	0.6792	0.6795	0.04
n_D^{20}	1.3853	1.3851	0.01
nbp, °C	98.38	98.427	0.05
<i>n</i> -Butyraldehyde			
$d_{4,25}^{25}$, g/mL	0.7964	0.7964	0.0
n_D^{25}	1.3767	1.3766	<0.01
nbp, °C	74.79	74.8	0.01
Isobutyraldehyde			
$d_{4,25}^{25}$, g/mL	0.7834	0.7836	0.03
n_D^{25}	1.3703	1.3727	0.17
nbp, ^c °C	68.87	64.1	0.35

^a Literature values taken from Riddick and Bunger.

^b % $\Delta = 100(\text{measd prop.} - \text{lit. prop.}) / (\text{lit. prop.})$. ^c Extrapolated from data in 40–51 °C range.

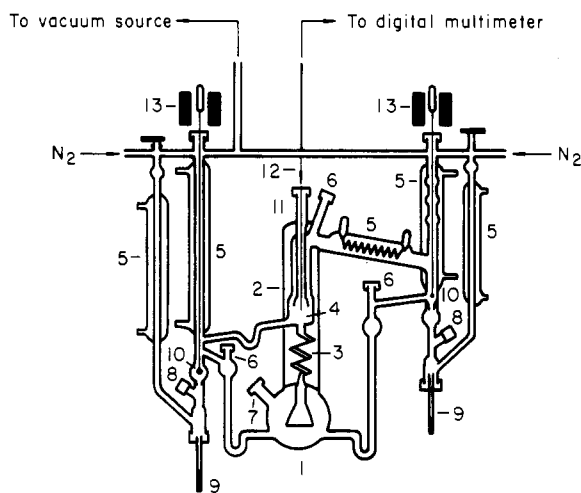


Figure 1. Detailed diagram of Stage-Muller still used in this work: (1) boiling flask, (2) vacuum jacket, (3) Cottrell pump, (4) equilibrium chamber, (5) condensers, (6) injection ports, (7) filling spout and thermometer well, (8) Teflon valves, (9) sample tubes, (10) glass ball valves, (11) equilibrium thermometer well, (12) equilibrium thermometer, (13) solenoid devices (actuates 10).

conditions, signified by stable temperature and pressure readings, usually required 60–90 min for the first data point and 45–60 min between points thereafter. In general, 2–4 days were needed to collect the 20 or so data points for a particular isotherm, not including the purification and gas-chromatograph calibration steps.

The equilibrium temperature was measured with a high-precision platinum resistance thermometer (Rosemount, Model 162N), whose calibration was traceable to the National Bureau

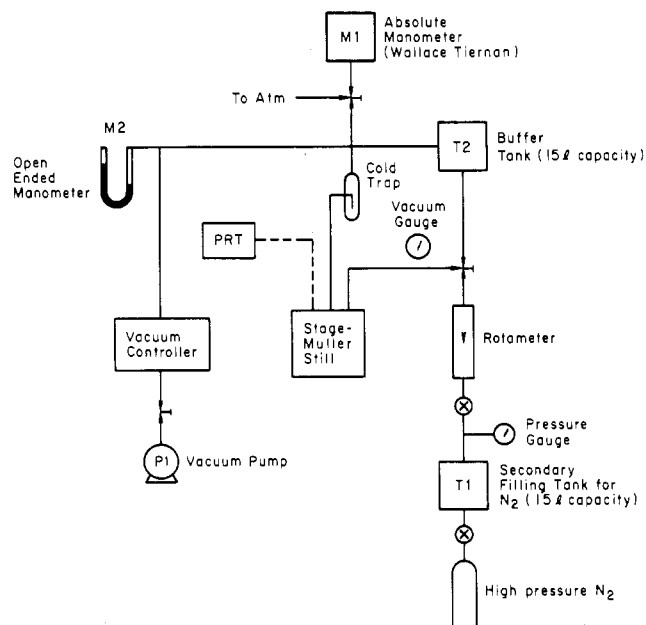


Figure 2. Overall schematic of experimental setup.

of Standards. The resistance was measured and converted to temperature by a programmable, digital multimeter (Fluke, Model 8520A) capable of 4-wire resistance measurement and accurate to 0.07% of the reading. The accuracy of this combination is better than 0.02 °C for the 0–100 °C range. The resolution of the temperature readings was 0.001 °C, which was advantageous for monitoring steady-state conditions.

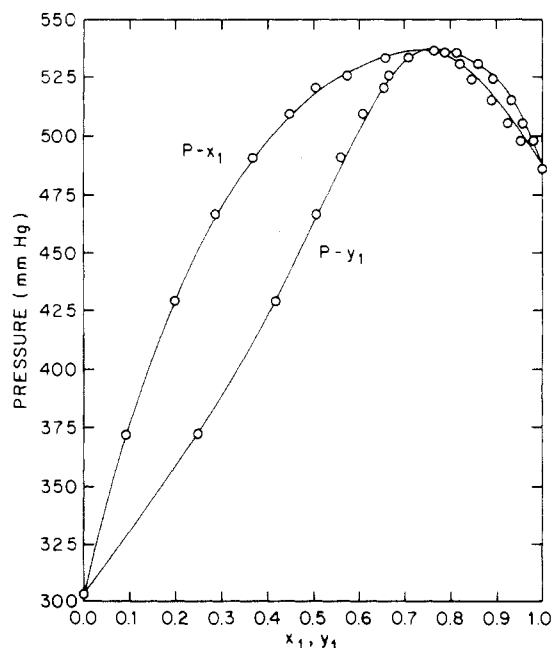
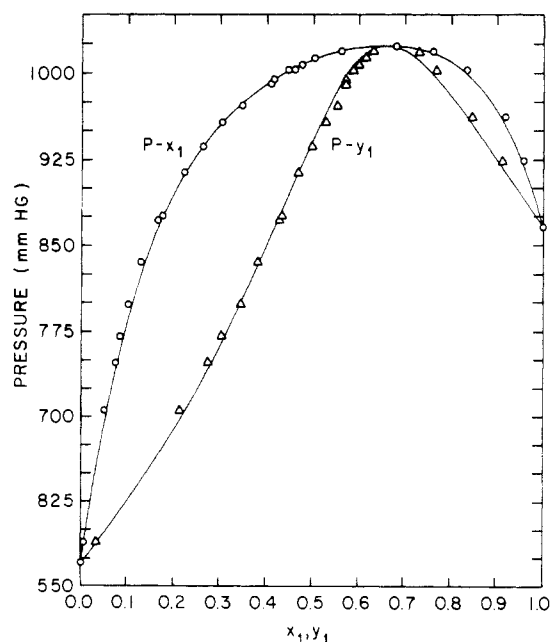
Pressure was measured with an accuracy of 0.16 mmHg by using a precision mercury manometer (Wallace and Tiernan, Model FA-187), whose flexible scale allowed compensation for local gravity and temperature effects. An electrical pressure regulator (manufactured by Fischer and supplied with the still) between the still and a vacuum pump maintained pressure constant to within 0.05 mmHg by means of a contact manometer and a solenoid valve.

The compositions of the collected liquid and condensed-vapor samples were determined by a gas chromatograph (Antek, Model 300), using a thermal conductivity detector. The chromatographic peaks were measured with an electronic integrator (Spectra-Physics Minigrator). A stainless steel column (6 ft long \times 1/4 in. i.d.), packed with 200 mesh Porapak Q, was used and operated isothermally from 175 to 220 °C, depending on the mixture being analyzed. Mole fractions were obtained from a calibration curve prepared from analyses of gravimetrically prepared samples. Each sample was analyzed at least 3 times. The relationship between response (area fraction) and composition (mole fraction) was fitted with a three-constant Redlich-Kister expansion. The constants were determined by a standard least-squares method. The accuracy of this method was found to be better than 0.5 mol %.

The accuracy of the results obtained with this equipment and operating procedure was established by reproducing previously published pure-component vapor pressure data (5) and binary vapor-liquid equilibrium data for the 1,2-dichloroethane/*n*-hep-

Table III. Vapor-Liquid Equilibrium Data for 1,2-Dichloroethane (1)/*n*-Heptane (2) at 70.00 °C

<i>P</i> , mmHg	<i>x</i> ₁	<i>y</i> ₁	<i>P</i> , mmHg	<i>x</i> ₁	<i>y</i> ₁
302.87	0.0000	0.0000	536.58	0.7644	0.7696
372.62	0.0911	0.2485	535.78	0.8132	0.7877
429.28	0.1979	0.4174	530.90	0.8603	0.8201
466.48	0.2867	0.5052	524.21	0.8930	0.8458
491.02	0.3674	0.5590	515.15	0.9332	0.8900
509.40	0.4467	0.6078	505.64	0.9572	0.9253
520.41	0.5044	0.6535	498.04	0.9812	0.9537
525.71	0.5733	0.6646	486.41	1.0000	1.0000
533.44	0.6578	0.7089			

Figure 3. *P*-*x*-*y* phase equilibrium diagram for 1,2-dichloroethane (1) and *n*-heptane (2) at 70.0 °C. The points are our smoothed data and the lines are the smoothed data of ref 6.Figure 4. *P*-*x*-*y* phase equilibrium diagram for *n*-pentane (1) and propionaldehyde (2) at 40.0 °C. The points O and Δ are the vapor and liquid compositions, and the line results from the Wilson equation fit of the data.Table IV. Vapor-Liquid Equilibrium Data for *n*-Pentane (1)/Propionaldehyde (2) at 40.00 °C

<i>P</i> , mmHg	<i>x</i> ₁	<i>y</i> ₁	<i>P</i> , mmHg	<i>x</i> ₁	<i>y</i> ₁
570.82	0.0000	0.0000	990.05	0.4082	0.5686
589.40	0.0059	0.0335	993.23	0.4135	0.5727
705.02	0.0503	0.2121	1001.80	0.4463	0.5877
747.81	0.0725	0.2747	1001.87	0.4600	0.5875
770.76	0.0835	0.3033	1006.40	0.4759	0.6002
798.40	0.1014	0.3452	1012.29	0.5031	0.6146
835.04	0.1272	0.3811	1017.88	0.5610	0.6311
871.90	0.1647	0.4288	1022.95	0.6812	0.6827
875.47	0.1746	0.4347	1017.76	0.7597	0.7293
913.19	0.2212	0.4685	1001.71	0.8333	0.7669
935.97	0.2615	0.4987	961.29	0.9180	0.8452
956.93	0.3019	0.5281	923.49	0.9577	0.9114
971.44	0.3476	0.5539	865.77	1.0000	1.0000

Table V. Vapor-Liquid Equilibrium Data for *n*-Butyraldehyde (1)/*n*-Heptane (2) at 45.00 °C

<i>P</i> , mmHg	<i>x</i> ₁	<i>y</i> ₁	<i>P</i> , mmHg	<i>x</i> ₁	<i>y</i> ₁
114.33	0.0000	0.0000	261.70	0.6761	0.7594
131.30	0.0288	0.1448	265.56	0.7535	0.7983
180.01	0.1270	0.4264	267.40	0.8134	0.8287
205.29	0.2159	0.5302	268.22	0.8498	0.8502
221.38	0.2979	0.5942	268.30	0.8865	0.8772
231.66	0.3577	0.6221	267.55	0.9245	0.9124
240.13	0.4291	0.6573	266.42	0.9585	0.9468
245.50	0.4743	0.6788	264.55	0.9860	0.9800
247.75	0.5010	0.6865	262.74	1.0000	1.0000
250.60	0.5434	0.7041			

Table VI. Vapor-Liquid Equilibrium Data for *n*-Butyraldehyde (1)/*n*-Heptane (2) at 70.00 °C

<i>P</i> , mmHg	<i>x</i> ₁	<i>y</i> ₁	<i>P</i> , mmHg	<i>x</i> ₁	<i>y</i> ₁
303.93	0.0000	0.0000	662.93	0.5613	0.7038
333.49	0.0227	0.1065	638.75	0.6416	0.7387
371.28	0.0575	0.2139	650.79	0.7211	0.7772
394.68	0.0857	0.2833	658.93	0.7850	0.8144
423.67	0.1195	0.3480	664.18	0.8376	0.8492
446.14	0.1465	0.3974	666.07	0.8638	0.8659
474.23	0.1893	0.4551	666.62	0.8902	0.8830
517.24	0.2645	0.5241	667.52	0.9222	0.9154
538.54	0.3074	0.5617	665.77	0.9533	0.9407
570.87	0.3767	0.6079	652.78	0.9922	0.9894
601.29	0.4755	0.6612	650.47	1.0000	1.0000

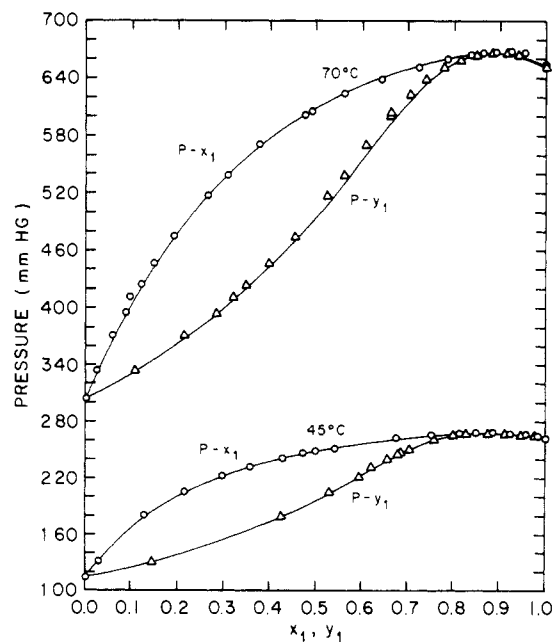
Figure 5. *P*-*x*-*y* phase equilibrium diagram for *n*-butyraldehyde (1) and *n*-heptane (2) at 45.0 and 70 °C. Legend as in Figure 4.

Table VII. Vapor-Liquid Equilibrium Data for Isobutyraldehyde (1)/*n*-Heptane (2) at 45.00 °C

<i>P</i> , mmHg	<i>x</i> ₁	<i>y</i> ₁	<i>P</i> , mmHg	<i>x</i> ₁	<i>y</i> ₁
114.33	0.0000	0.0000	336.25	0.5843	0.7938
149.37	0.0348	0.2550	345.10	0.6284	0.8116
187.03	0.0846	0.4292	356.43	0.7043	0.8404
225.09	0.1583	0.5523	364.64	0.7636	0.8626
257.76	0.2420	0.6344	371.13	0.8167	0.8842
285.02	0.3312	0.6924	377.06	0.8616	0.9074
303.06	0.4073	0.7266	381.41	0.9020	0.9301
310.53	0.4373	0.7426	386.36	0.9562	0.9641
315.63	0.4669	0.7499	388.68	0.9833	0.9839
328.98	0.5319	0.7786	389.97	1.0000	1.0000

tane system at 70 °C (6), as described below.

Experimental Results and Discussion

Isothermal measurements were made for 1,2-dichloroethane/*n*-heptane at 70 °C, *n*-pentane/propionaldehyde at 40 °C, heptane/*n*-butyraldehyde at 45 and 70 °C, and isobutyraldehyde/*n*-heptane at 45 °C. The raw (unsmoothed) data are presented in Tables III–VII and plotted in Figures 3–6. The thermodynamic consistency of the data was checked by the point-to-point test of Van Ness et al. (7) as modified by Fredenslund et al. (8), which allows analysis of individual data points. The consistency was considered good for the suggested criterion of $AAD(\Delta y) < 0.010$ (8) for consistent data (see Table VIII).

As can be seen from Figure 3, the data measured for 1,2-dichloroethane/*n*-heptane at 70 °C in this study agree well with the data reported by Gutsche and Knapp (6). The values for the $AAD(\Delta y)$ from the point-to-point consistency test for the two data sets (see Table VIII) are considered very good. The low-boiling azeotropic point estimated from our data is also comparable to that determined by Gutsche and Knapp, as shown in Table IX. The azeotropic points were estimated from the best-fit model in both cases.

Moderately positive deviations from ideality were observed for each of the aldehyde/hydrocarbon systems. Minimum-boiling azeotropes were formed in all but the isobutyraldehyde/*n*-heptane system. An azeotrope does not occur in this last system because of the larger difference in the vapor pressures of the pure components. The azeotropic points were calculated by using the activity coefficient which gave the best fit (see below) and are presented in Table IX.

Activity Coefficients and Models

The experimental activity coefficient for component *i*, γ_i , was calculated for each data point by using

$$\gamma_i = (y_i \phi_i P) / (x_i f_i^\circ) \quad (2)$$

Table VIII. Results of Point-to-Point Consistency Test

system	<i>T</i> , °C	gas phase	<i>N</i>	$AAD(\Delta y)$	$AAD(\Delta P)$, mmHg	consistency ^a
1,2-dichloroethane/ <i>n</i> -heptane (Gutsche)	70.0	real	18	0.0051	0.75	+
1,2-dichloroethane/ <i>n</i> -heptane (this study)	70.0	real	17	0.0048	0.83	+
<i>n</i> -pentane/propionaldehyde	40.0	ideal	26	0.0070	1.31	+
<i>n</i> -butyraldehyde/ <i>n</i> -heptane	45.0	real	19	0.0055	0.45	+
<i>n</i> -butyraldehyde/ <i>n</i> -heptane	70.0	real	22	0.0068	0.98	+
isobutyraldehyde/ <i>n</i> -heptane	45.0	real	19	0.0021	0.37	+

^a The data are considered consistent (+) if $AAD(\Delta y) \leq 0.01$ (3).

Table IX. Estimated Azeotropic Points

system	<i>T</i> , °C	<i>x</i> ₁ ^{az}	<i>P</i> ^{az} , mmHg	model	<i>A</i> ₁₂	<i>A</i> ₂₁
1,2-dichloroethane/ <i>n</i> -heptane (Gutsche)	70.0	0.749	537.22	UNIQUAC	85.006	1004.42
1,2-dichloroethane/ <i>n</i> -heptane (this study)	70.0	0.746	536.46	Van Laar	0.8400	1.2610
<i>n</i> -pentane/propionaldehyde	40.0	0.656	1023.25	Wilson	0.4160	0.4458
<i>n</i> -butyraldehyde/ <i>n</i> -heptane	45.0	0.876	267.99	Wilson	0.5405	0.5082
<i>n</i> -butyraldehyde/ <i>n</i> -heptane	70.0	0.880	664.61	Wilson	0.8148	0.3932

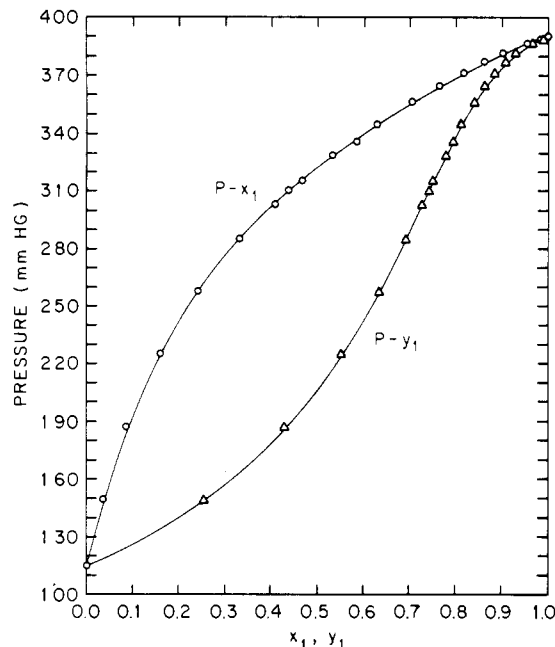


Figure 6. *P*-*x*-*y* phase equilibrium diagram for isobutyraldehyde (1) and *n*-heptane (2) at 45 °C. Legend as in Figure 4.

where x_i and y_i are the liquid and vapor mole fractions of species *i*, respectively, and ϕ_i is its vapor-phase fugacity coefficient. The fugacity coefficients were calculated from the virial equation, truncated after the second term

$$\ln \phi_i = P/RT \left(\sum_j y_j B_{ij} - B_{ii} \right) \quad (3)$$

The second virial coefficients, *B*, were obtained by the method of Hayden and O'Connell (9). The standard-state fugacity, f_i° (that is, the fugacity of pure liquid *i* at the system temperature and pressure), is given by

$$f_i^\circ = \phi_i^s f_i^s \exp[v_i(P - P_i^s)/RT] \quad (4)$$

The form of the Poynting correction factor, $\exp[v_i(P - P_i^s)/RT]$, for the effect of pressure on f_i° assumes that the liquid molar volume, v_i , is independent of pressure. The liquid molar volumes were calculated from the COSTALD method (10).

The activity coefficients calculated in this manner were correlated by fitting the three-suffix Margules (11), Van Laar (11), Wilson (12) NRTL (13), and UNIQUAC (14) activity coefficient models for each isotherm. The two adjustable parameters for each model (the α parameter in the NRTL model was fixed at 0.3) were estimated by using the maximum like-

Table X. Estimated Parameters from Data Correlation

$T, ^\circ\text{C}$	model	parameters ^{a,b}		σ_F^c	AAD(Δy)	AAD(ΔP), mmHg
		A_{12}	A_{21}			
<i>n</i> -Pentane/Propionaldehyde						
40	Margules	1.3381	-0.0025	2.92	0.0084	6.35
	Van Laar	1.2465	1.4037	4.36	0.0099	10.06
	Wilson	0.41597	0.44583	1.79	0.0085	3.48
	NRTL	1920.1	2007.6	2.63	0.0083	5.61
	UNIQUAC	2021.5	365.3	4.54	0.0097	10.32
<i>n</i> -Butyraldehyde/ <i>n</i> -Heptane						
45	Margules	1.0835	0.0302	1.37	0.0068	0.82
	Van Laar	1.0526	1.1153	1.36	0.0068	0.81
	Wilson	0.5405	0.5082	0.98	0.0061	0.60
	NRTL	1715.1	1439.7	1.31	0.0063	0.77
	UNIQUAC	-383.9	1458.4	1.34	0.0068	0.79
<i>n</i> -Butyraldehyde/ <i>n</i> -Heptane						
70	Margules	0.9244	0.1512	3.31	0.0084	3.21
	Van Laar	0.7858	1.1002	2.91	0.0083	2.92
	Wilson	0.8143	0.3932	2.55	0.0078	2.37
	NRTL	1496.2	1550.1	6.98	0.0084	6.94
	UNIQUAC	156.86	709.4	2.88	0.0083	2.87
Isobutyraldehyde/ <i>n</i> -Heptane						
45	Margules	0.9952	0.0045	1.63	0.0056	1.50
	Van Laar	0.9905	0.9999	1.63	0.0056	1.50
	Wilson	0.5459	0.5701	1.22	0.0045	1.13
	NRTL	1444.5	1423.1	1.52	0.0053	1.41
	UNIQUAC	-492.0	1526.5	1.62	0.0057	1.49

^a The standard deviations used in the maximum likelihood method were $\sigma_x = 0.003$, $\sigma_y = 0.005$, $\sigma_P = 0.5$ mmHg, $\sigma_T = 0.02$ °C. ^b Wilson: $A_{12} = \lambda_{12} - \lambda_{11}$, $A_{21} = \lambda_{21} - \lambda_{22}$. NRTL: $A_{12} = g_{12} - g_{22}$, $A_{21} = g_{21} - g_{11}$ (J/mol). UNIQUAC: $A_{12} = u_{12} - u_{22}$, $A_{21} = u_{21} - u_{11}$ (J/mol). ^c $\sigma_F = [F/(n-2)]^{1/2}$.

likelihood method, which accounts for experimental error in all variables (T , P , x , and y), by minimizing the following objective function:

$$S = \sum_j \left[\frac{\sigma(F_2)F_1}{\sigma} \right]^2 + \sum_j \left[\frac{\sigma(F_1)F_2}{\sigma} \right]^2 + 2 \sum_j \left[\frac{\sigma(F_1, F_2)F_1 F_2}{\sigma^2} \right] \quad (5)$$

where $\sigma = \sigma(F_1)\sigma(F_2) - \sigma(F_1, F_2)$ and N = number of experimental points. The standard deviations in eq 5 are obtained by the propagation of error law (15). The following equations for F_1 and F_2 , as suggested by Kemeny and Manczinger (15), were used:

$$F_1 = p^{\text{exptl}} - p^{\text{calcd}} = p^{\text{exptl}} - \sum_i x_i \gamma_i^0 \phi_i \quad (6)$$

$$F_2 = \ln(\gamma_1^{\text{exptl}}/\gamma_2^{\text{exptl}}) - \ln(\gamma_1^{\text{calcd}}/\gamma_2^{\text{calcd}}) = \ln(\gamma_1^{\text{exptl}}/\gamma_2^{\text{exptl}}) - \ln([y_1 \phi_1 x_2 f_2]/[y_2 \phi_2 x_1 f_1]) \quad (7)$$

The results of the parameter estimation for each model are given in Table X. A lower value of the standard deviation of the minimized sum of squares of eq 5, σ_s , indicates a better representation of the data given by a model. In this study, the Wilson equation resulted in the lowest value of σ_s for all four data sets. However, an F -test (16) at the 95% confidence level revealed this difference to be statistically significant only for the *n*-pentane/propionaldehyde data.

In Figure 7 are presented the excess Gibbs free energies as a function of composition for each of the systems studied as derived from experiment using

$$G^e(x_1, x_2, T) = RT[x_1 \ln \gamma_1 + x_2 \ln \gamma_2] \quad (8)$$

and from the best-fit thermodynamic model. It is interesting to note that the excess Gibbs free energy vs. composition curves for all the aldehyde/hydrocarbon systems are very similar in size and shape.

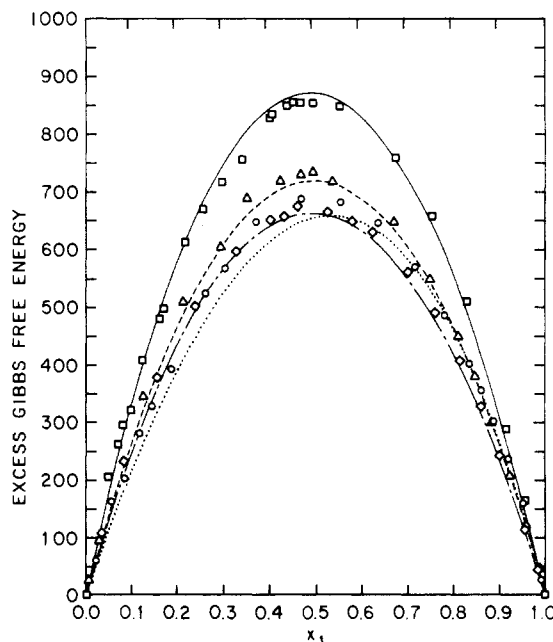


Figure 7. Excess Gibbs free energies in J/mol as a function of composition for each of the aldehyde/hydrocarbon systems studied here: *n*-pentane and propionaldehyde at 40 °C (\square and —); *n*-butyraldehyde and *n*-heptane at 45 °C (Δ and ---) and at 70 °C (\circ and ...); and isobutyraldehyde and *n*-heptane at 45 °C (\diamond and -.-). In each case the points are derived from the experimental data and the lines are the Wilson equation fit.

In addition, new group interaction parameters of the UNIFAC method were estimated from the data of this study for aldehyde (CHO)/hydrocarbon (CH₂) interactions by the method described by Fredenslund et al. (8), based on minimizing the following objective function:

$$F = \sum_j \left[\ln \gamma_i^{\text{exptl}} - \ln \gamma_i^{\text{UNIFAC}} \right]^2 \quad (9)$$

Table XI. New Group Interaction Parameters for UNIFAC and Comparison with the Old Parameters

	old parameters ^a	new parameters ^b
AAD($\Delta\gamma_1/\gamma_1$)	0.050	0.038
AAD($\Delta\gamma_2/\gamma_2$)	0.033	0.020

^a $a(\text{CH}_2/\text{CHO}) = 677.00$, $a(\text{CHO}/\text{CH}_2) = 505.70$.
^b $a(\text{CH}_2/\text{CHO}) = 618.8$, $a(\text{CHO}/\text{CH}_2) = 2261.0$.

The new parameters are shown in Table XI, along with the comparison of activity coefficients calculated from both the previous parameters based only on propionaldehyde/cyclohexane data (17), and the new parameters. As might be expected, the fit of the *n*-butyraldehyde and isobutyraldehyde data is better with the new parameters but is worse for the mixture containing propionaldehyde. Clearly, to obtain the best possible parameters for the aldehyde/hydrocarbon functional-group interactions, a regression of data for many systems is needed.

Conclusions

Previously unavailable vapor-liquid equilibrium data for three aldehyde/hydrocarbon systems were measured. These data are themselves of potential use in engineering design and also will be of use in the estimation of more accurate group interaction parameters in the UNIFAC method and other functional-group methods for CHO-CH₂ and CH₂-CHO interactions. Minimum-boiling azeotropes were observed for the *n*-pentane/propionaldehyde system at 40 °C and the *n*-butyraldehyde/*n*-heptane system at 45 and 70 °C.

Acknowledgment

We thank Dr. B. Gutsche and Professor H. Knapp (Technical University of Berlin) for their advice and assistance in setting up the experimental equipment used here.

Glossary

<i>A</i> , <i>B</i> , <i>C</i>	Antoine constants (eq 1)
<i>B</i>	second virial coefficient, J/g-mol
<i>C</i>	number of components
<i>d</i> ₄	density relative to that of water at 4 °C, g/mL
<i>f</i>	standard-state fugacity of liquid (eq 4), mmHg
<i>G</i> ^o	excess Gibbs free energy, J/mol
<i>n</i> _D	refractive index
<i>P</i>	total pressure, mmHg
<i>R</i>	gas constant
<i>T</i>	temperature, °C

<i>v</i>	molar liquid volume, cm ³ /g-mol
<i>x</i>	liquid-phase mole fraction
<i>y</i>	vapor-phase mole fraction
γ	activity coefficient
ϕ	fugacity coefficient (eq 3)
σ	standard deviation
Δ	difference between the experimental and calculated values
AAD	absolute average deviation
rmsd	root mean square deviation
nbp	normal boiling point, °C
Subscripts	
<i>i</i>	component <i>i</i>
Superscripts	
exptl	experimentally measured value
calcd	calculated value
s	saturation value
o	reference-state value

Registry No. *n*-Pentane, 109-66-0; propionaldehyde, 123-38-6; *n*-heptane, 142-82-5; *n*-butyraldehyde, 123-72-8; isobutyraldehyde, 78-84-2.

Literature Cited

- (1) Smith, T.; Bonner, H. *Ind. Eng. Chem.* **1951**, *43*, 1169.
- (2) Hala, E.; Pick, J.; Fried, V.; Viliam, O. "Vapor-Liquid Equilibrium"; Pergamon Press: New York, 1967; pp 171-8.
- (3) Malanowski, S. "Vapor-Liquid Equilibrium"; PNW: Warsaw, 1974.
- (4) Stage, H.; Fischer, W. G. *Glas + Instrum.-Tech.* **1968**, 1167.
- (5) Riddick, J. A.; Bunger, E. B. "Organic Solvents. Physical Properties and Methods of Purification"; Wiley-Interscience: New York, 1970.
- (6) Gutsche, B.; Knapp, H. *Fluid Phase Equil.* **1982**, *8*, 285-300.
- (7) Van Ness, H. C.; Byer, S. M.; Gibbs, R. E. *AIChE J.* **1973**, *19*, 238-44.
- (8) Fredenslund, A.; Gmehling, J.; Rasmussen, P. "Vapor-Liquid Equilibrium Using UNIFAC"; Elsevier: Amsterdam, 1977; pp 68-74.
- (9) Hayden, J. G.; O'Connell, J. P. *Ind. Eng. Chem., Process Des. Dev.* **1975**, *14*, 209.
- (10) Hankinson, R. W.; Thompson, G. H. *AIChE J.* **1975**, *25*, 653.
- (11) Sandler, S. I. "Chemical and Engineering Thermodynamics"; Wiley: New York, 1977; Chapter 7.
- (12) Wilson, G. M. *J. Am. Chem. Soc.* **1964**, *86*, 127-30.
- (13) Renon, H.; Prausnitz, J. M. *AIChE J.* **1968**, *14*, 135-44.
- (14) Abrams, D. S.; Prausnitz, J. M. *AIChE J.* **1975**, *21*, 116-28.
- (15) Kemeny, S.; Manczinger, J.; Skjold-Jorgensen, S.; Toth, K. *AIChE J.* **1982**, *28*, 20-30.
- (16) Brownlee, K. A. "Statistical Theory and Methodology in Science and Engineering"; Wiley: New York, 1965.
- (17) Matsunaga, I.; Katayama, T. *J. Chem. Eng. Jpn.* **1973**, *6*, 397.

Received for review March 24, 1983. Accepted September 15, 1983. The equipment for this work was purchased with funds provided by NSF Grant CPE 8104553 to the University of Delaware and also funds from the Mobil Foundation. R.E. also is pleased to acknowledge the financial support that he received as a graduate student from the Department of Chemical Engineering of the University of Delaware.

Excess Volumes of 1,1,2,2-Tetrachloroethane + Ketone

Nettem V. Choudary, Jyoti C. Mouli, A. Krishnalal,* and P. R. Naidu

Sri Venkateswara University Chemical Laboratories, Tirupati 517 502, India

Excess volumes for the binary mixtures of 1,1,2,2-tetrachloroethane with methyl ethyl ketone, diethyl ketone, and methyl propyl ketone have been measured at 303.15 and 313.15 K. V^E is negative over the entire mole fraction range in all the mixtures. The negative excess volumes have been explained in terms of dipole-induced dipole interactions.

Introduction

Many attempts have been made to study molecular interactions in mixtures containing chloroalkanes (1-4) and ketones (5-8) as the components. Various thermodynamic and nonthermodynamic techniques have been used to provide evidence for the existence of weak specific interactions in the mixtures of ketones and chloroalkanes (9-11). The electron-